OPEN ACCESS Freely available online

PLOS | COMPUTATIONAL BIOLOGY

Estimating the Probability of Polyreactive Antibodies 4E10 and 2F5 Disabling a gp41 Trimer after T Cell-HIV Adhesion

Bin Hu[1], Hua-Xin Liao[2], S. Munir Alam[2], Byron Goldstein[1]*

1 Theoretical Biology and Biophysics Group, Theoretical Division, Los Alamos National Laboratory, Los Alamos, New Mexico, United States of America, **2** Human Vaccine Institute, Duke University Medical Center, Durham, North Carolina, United States of America

Abstract

A few broadly neutralizing antibodies, isolated from HIV-1 infected individuals, recognize epitopes in the membrane proximal external region (MPER) of gp41 that are transiently exposed during viral entry. The best characterized, 4E10 and 2F5, are polyreactive, binding to the viral membrane and their epitopes in the MPER. We present a model to calculate, for any antibody concentration, the probability that during the pre-hairpin intermediate, the transient period when the epitopes are first exposed, a bound antibody will disable a trivalent gp41 before fusion is complete. When 4E10 or 2F5 bind to the MPER, a conformational change is induced that results in a stably bound complex. The model predicts that for these antibodies to be effective at neutralization, the time to disable an epitope must be shorter than the time the antibody remains bound in this conformation, about five minutes or less for 4E10 and 2F5. We investigate the role of avidity in neutralization and show that 2F5 IgG, but not 4E10, is much more effective at neutralization than its Fab fragment. We attribute this to 2F5 interacting more stably than 4E10 with the viral membrane. We use the model to elucidate the parameters that determine the ability of these antibodies to disable epitopes and propose an extension of the model to analyze neutralization data. The extended model predicts the dependencies of IC_{50} for neutralization on the rate constants that characterize antibody binding, the rate of fusion of gp41, and the number of gp41 bridging the virus and target cell at the start of the pre-hairpin intermediate. Analysis of neutralization experiments indicate that only a small number of gp41 bridges must be disabled to prevent fusion. However, the model cannot determine the exact number from neutralization experiments alone.

Citation: Hu B, Liao H-X, Alam SM, Goldstein B (2014) Estimating the Probability of Polyreactive Antibodies 4E10 and 2F5 Disabling a gp41 Trimer after T Cell-HIV Adhesion. PLoS Comput Biol 10(1): e1003431. doi:10.1371/journal.pcbi.1003431

Editor: Rustom Antia, Emory University, United States of America

Received August 15, 2013; **Accepted** November 25, 2013; **Published** January 30, 2014

Funding: The research reported in this publication was supported by the National Institute of General Medical Sciences of the National Institutes of Health under award number R37-GM035556 and by the Department of Energy contract DEAC52-06NA25396. The content is solely the responsibility of the authors and does not necessarily represent the official views of the National Institutes of Health. The funders had no role in study design, data collection and analysis, decision to publish, or preparation of the manuscript.

Competing Interests: The authors have declared that no competing interests exist.

* E-mail: bxg@lanl.gov

Introduction

A small but growing number of HIV-1 broadly neutralizing monoclonal antibodies (mAbs) have been isolated from HIV-1 infected individuals (reviewed in [1]). A subset of these (4E10, 2F5, m66.6 and Z13e1) bind to epitopes at the base of gp41, along a segment adjacent to the viral membrane known as the membrane proximal external region (MPER) that links the gp41 transmembrane domain to its ectodomain [2,3]. Two, 4E10 and 2F5, have been extensively characterized. Each has been shown to be polyreactive [4–6], with an elongated heavy chain complementarity determining region 3 (CDRH3) that has a hydrophobic surface that does not contact the peptide antigen [7,8], but that contributes to the ability of 4E10 and 2F5 to bind to the virion membrane and to broadly neutralise [9–13]. Recently, self-antigens have been identified that these antibodies recognize [14]. Of the two mAbs, 2F5 interacts more strongly with membrane as demonstrated by its ability to bind to virus-like particles bearing no envelop glycoprotein (Env spikes) [6].

Detailed structural studies and surface plasmon resonance measurements (SPR) have shown that the epitopes for 4E10 and 2F5 are within the MPER, lying along the viral surface with parts immersed in the viral membrane [15–17]. The binding of these antibodies to their epitopes on the viral membrane appears to be step-wise [4,17,18] with the membrane associated antibody and the MPER undergoing conformaional changes [15,16,18] that result in a more stably bound complex [4,8,17,18]. For both mAbs and their Fabs, the rate constants that describe the kinetics of the two step process have been determined for binding to liposome-gp41 peptide conjugates [4].

The epitopes recognized by 4E10 and 2F5 on gp41 are displayed on the viral membrane after the binding of HIV-1 to the target cell has occurred and the processes that result in membrane fusion have begun [2]. This stage, between pre- and postfusion, called the pre-hairpin intermediate [19], has a lifetime that has been estimated to range from a few seconds to many minutes [20–23]. The tenet that 4E10 and 2F5 only recognize epitopes on the MPER during the pre-hairpin intermediate appears to strictly hold only for HIV-1 isolates that are highly resistant to neutralization [24]. For HIV-1 isolates that are less resistant to neutralization, the MPER epitopes may be accessible to antibody binding before the pre-hairpin intermediate stage has been initiated. Alternatively,

Author Summary

Most people who become infected with HIV generate a strong antibody response to the infecting virus population. Unfortunately, the protection offered by the antibody is short lived as the virus rapidly mutates and renders the antibodies impotent in preventing further infection. There are a few antibodies, however, that have been isolated from infected individuals that can block infection by many different viral strains. Among these are several that target sites on the HIV that are exposed only after the virus has attached to a cell. These antibodies have a brief window of time to prevent fusion of the virus and cell. They are special in that they bind both to the viral membrane and to sequences on the gp41 protein that lie along the viral surface. Here, we present a model that predicts the concentrations at which these antibodies effectively neutralize the virus. The model tells us what properties of antibody binding are key in determining efficient neutralization and what properties have little influence. A prediction of the model is that in a standard neutralization assay there are only a small number of attachments between virus and cell and disabling these is sufficient to prevent infection.

enhanced susceptibility to MPER neutralizing antibodies could be a result of prolonged exposure of the intermediate state during viral entry [25].

Although numerous studies have determined rate constants for the binding of 4E10 and 2F5 to peptide epitopes in solution and peptides conjugated to liposomes [2,4,10,12,13,15,17,18], and estimates of the lifetime of the exposure of the MPER on HIV-1 have been obtained [20–22,26], a quantitative description of how these parameters determine the mAb concentrations that are effective in inhibiting fusion has been lacking. Here we present a model that allows us to calculate, as a function of the serum antibody concentration, the probability of a trivalent MPER being disabled by polyreactive mAbs.

A question we also consider is how the probability of disabling a single epitope is related to the probability of blocking membrane fusion of HIV-1 and target cell when, at the start of the pre-hairpin intermediate stage, N epitopes bridge the two membranes. We present a model that predicts the form of a neutralization curve, i.e., the percent neutralization versus the antibody or Fab concentration, and how the IC_{50} for neutralization depends on N, as well as on the rate constants that characterize antibody binding and the rate of fusion of gp41. We use the model to fit neutralization experiments where neutralization is achieved with either 4E10 or 2F5 IgG or Fab. Our analysis of these experiments indicates that at the start of the pre-hairpin intermediate only a few gp41 trimers are involved in bridging the virion and target cell. As the bonds break sequentially those that remain come under additional strain and are disabled more easily.

Results

We present a model to calculate the probability p_b of an epitope that is only present in the pre-hairpin intermediate being disabled by a mAb or Fab at a solution concentration A. The model starts at time $t=0$ when binding between a target cell and an HIV has occurred and the epitope in the MPER first becomes accessible on the viral surface. This opens a window in time for the antibody to bind and prevent fusion. The antibodies we consider are polyreactive with a single Fab site being able to recognize both a subset of lipids on the HIV surface and the exposed epitope. We define the mean lifetime the epitope remains exposed before membrane fusion occurs to be $1/\lambda$. Once fusion occurs, blocking infection by an antibody is no longer possible. At time $t=0$ there are $E_0(0)$ exposed epitopes on the viral surface. At a time t later $E_f(t)$ of these have fused, where

$$E_f(t)=\lambda\int_0^t E_0(t')dt' \tag{1}$$

The fraction of epitopes $f(t)$ that fuse by time t is

$$f(t)=E_f(t)/E_0(0) \tag{2}$$

For any single epitope, the probability of it fusing with the target cell it is bound to before it is disabled by a bound antibody is equal to $f(\infty)$. The probability of this fusion being prevented by an antibody is

$$p_b=1-f(\infty) \tag{3}$$

The probability p_b of disabling a gp41 trimer in the pre-hairpin intermediate may depend on both A, the mAb concentration and on N, the number of gp41 trimers that span the virus and target cell. For example when there is only a single bond remaining the strain on the bond may be sufficient to cause spontaneous rupture. At a fixed antibody concentration, we expect p_b to decrease (becomes harder to break a bond) as the number of gp41 increases until p_b becomes independent of N. We first calculate p_b in this limit when there is a uniform distribution of gp41 trimers bridging the virus and target cell and p_b is independent of N. When we analyze neutralization experiments we will consider how p_b depends on N when N is small.

To obtain an expression for p_b, we assume the following:

1. In the absence of mAb or Fab bound to the MPER, fusion is irreversible once the pre-hairpin intermediate is reached.
2. Fusion is blocked as long as a mAb or Fab is bound to a site in the MPER.
3. If the mAb or Fab remains bound to the site for a sufficient time the epitope is rendered nonfunctional. This may be the result of the mAb or Fab inducing an irreversible structural change in gp41 with the concomitant shedding of gp120 [27], or through some other mechanism. If the mAb or Fab dissociates before disabling occurs, the processes leading to fusion can proceed with the rates remaining unchanged.
4. When a mAb or Fab binds to an epitope it induces a conformational change that results in the formation of a stably bound complex [4,17,18]. The binding kinetics of Fab or mAb is well described by a two step process characterized by four rate constants.
5. Up to three Fab can bind to the three gp41s in a spike [28,29] with the binding being independent of the bound states of the neighboring gp41, i.e., we assume that there is no cooperativity between bound gp41 in the same spike.
6. Only one 2F5 or 4E10 mAb can bind to the three gp41s in a spike [28].
7. A 2F5 or 4E10 mAb can't simultaneously bind two MPERs in the same spike nor can it bind two MPERs on different spikes. (The latter assumption is equivalent to assuming the spikes are immobile in the HIV membrane and the subset of spikes that are bound to a T cell have nearest neighbor distances that are longer than an antibody can span [30,31]).

8. In a neutralization experiment we assume that the mAb or Fab concentration A is in large excess compared to the number of epitopes exposed so that the binding to epitopes causes a negligible depletion of the mAb or Fab solution concentration. Further, we assume that any binding of mAb or Fab directly to the membrane minimally depletes their solution concentration.

As indicated above (4.) we describe the Fab or IgG binding to epitopes in the MPER on the surface of a virion by a two-step process. However, depending on the model, the interpretation of these rate constants will differ. At least two models, the encounter model and the wedging model, have been proposed for how 2F5 and 4E10 can form a stable complex with an MPER on the virion membrane (outlined in Figure 11 of [13]). In the encounter model, the first step encompasses the antibody associating with the membrane and then, through a surface interaction, binding to the exposed MPER residues. In the second step a conformational change is induced in the MPER that results in a long-lived bound complex [4]. In the wedging model, in the first step the antibody binds simultaneously to the membrane and the MPER that is partially embedded in the membrane. This results in the pulling of the MPER partially out of the membrane and the formation of a long-lived bound complex [13,15,16,18].

Inhibition by polyreactive Fab

We first consider a polyreactive Fab at low concentration that can bind to both a site in the MPER and to lipids in the membrane. The binding reactions that the Fab can undergo in the model and their rate constants are illustrated in Figure 1. The parameters of the model are summarized in Table 1. By the low concentration limit we mean that at most one Fab can be bound to a spike, even though the spike contains three gp41 binding sites for the Fab. After we explore this limit we treat the general case where up to three Fab can be bound to one spike. We assume it takes only one Fab bound for a sufficient time to an MPER to disable a spike, i.e. we take the stoichiometry of trimer neutralization to be one [32]. We use the term spike and epitope interchangeably in what follows, so in the model an epitope is composed of three gp41 with each containing a single binding site for the Fab. A free epitope has all three sites free.

In the model free epitope with surface concentration E_0 is lost through fusion with rate λ. Free epitope is also lost when a Fab, with solution concentration A, binds to the epitope. Free epitope is gained when a Fab bound to an epitope with surface concentration E_1 dissociates from the epitope. A bound Fab can induce a conformational change leading to the formation of long-lived complexes with surface concentration E_T [4,15,17]. A Fab bound in this way for a sufficient time can render the epitope nonfunctional [30]. This conversion to a nonfunctional state takes a mean time equal to $1/d_T$. Since the mean lifetime of an epitope bound to a 4E10 or 2F5 Fab or IgG before it undergoes a conformational change is short $\approx$5–20 s ([4], Table 2), we expect there to be negligible disabling of epitopes before the conformational change occurs. We therefore take disabling of the epitope to occur only after a stable complex has formed. In the low Fab concentration limit the following set of ordinary differential equations (ODEs) describes the kinetics of the epitope in the presence of Fab. The initial conditions for these equations are that at t = 0, when the MPER first becomes accessible, $E_0 = E_0(0)$, $E_1 = 0$ and $E_T = 0$.

$$dE_0/dt = -\lambda E_0 - 3k_{+e}AE_0 + k_{-e}E_1 \qquad (4)$$

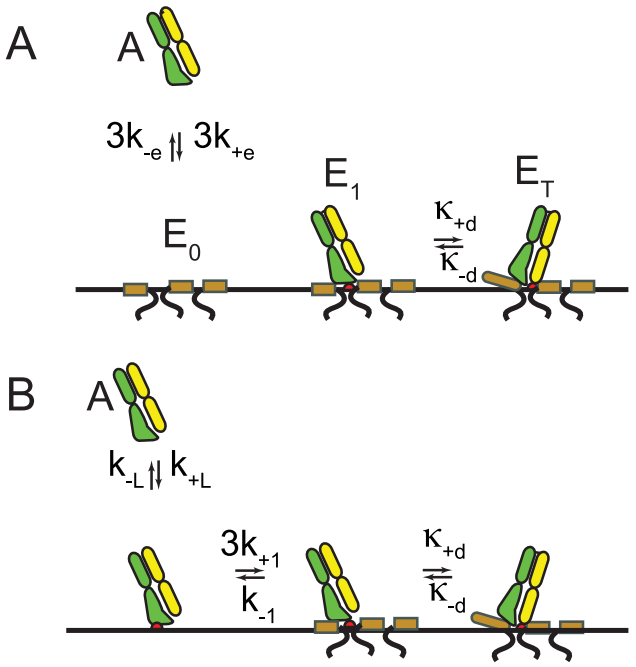

Figure 1. A. Two step binding scheme for a polyreactive Fab binding to an epitope. The epitope is exposed transiently for a mean time $1/\lambda$ before virion and target cell membranes fuse and infection becomes irreversible. Only the transmembrane domain and the MPER on the viral membrane are pictured. The remainder of gp41, which extends into the target cell membrane, is not shown. The first step, binding from solution to the MPER on the virion surface is described by rate constants k_{+e} and k_{-e}. The second step, an induced conformational change resulting in a long-lived Fab-MPER complex, is described by intramolecular rate constants κ_{+d} and κ_{-d}. The model assumes that if an Fab remains bound to the MPER after the conformational change for a sufficient time $(1/d_T)$ the epitope is disabled. B. In the encounter model the Fab binds first to lipids on the membrane with rate constants k_{+L} and k_{-L}, then diffuses to the MPER and reacts with surface rate constants k_{+1} and k_{-1}. Because binding to the lipid is weak and rapidly reversible we show in **SI1** of Text S1 that for this model $k_{+e} = K_L L k_{+1}$ and $k_{-e} = k_{-1}$. Here $K_L = k_{+L}/k_{-L}$ is the lipid equilibrium constant and L is the surface concentration of lipid binding sites.
doi:10.1371/journal.pcbi.1003431.g001

$$dE_1/dt = 3k_{+e}AE_0 - k_{-e}E_1 - \kappa_{+d}E_1 + \kappa_{-d}E_T \qquad (5)$$

$$dE_T/dt = \kappa_{+d}E_1 - \kappa_{-d}E_T - d_T E_T \qquad (6)$$

We only need the solution of these equations at $t = \infty$ after all epitopes have either fused or been disabled (see Eq. (3)). The solution of Eqs (4)–(6) for $E_0(\infty)$ is given in **SI2** of Text S1, the Supporting information. Substitution of the expression we obtain for $E_0(\infty)$ into Eq. (3) gives us the desired expression for p_b

$$p_b = \frac{\delta A}{\lambda + \delta A} \qquad (7)$$

The parameter δ is an effective three-dimensional forward rate constant given in terms of the rate constants for the reversible binding of the Fab to the epitope, k_{+e} and k_{-e}, and the rate constants for the reversible transition induced by the Fab binding to the epitope, κ_+ and κ_-. In addition, δ depends on the mean

Table 1. Definition of the parameters of the model.

parameter	description
N	The initial number of gp41 bridging virus and target cell
IC_{50}	antibody conc. at which 50% neutralization achieved (M)
p_b	probability a gp41 in the presence of a large number of other gp41 is disabled before fusion
p_i	probability a gp41 in the presence of $i-1$ other gp41 is disabled before fusion
A	mAb or Fab solution concentration (M)
λ	rate of gp41 fusion in the absence of mAb or Fab (s^{-1})
$E_0(0)$	surface conc. of unbound gp41 at $t=0$ (number/cm^2)
$E_f(t)$	conc. of gp41 that have fused by time t (number/cm^2)
$f(t)$	fraction of gp41 that have fused by time t
$E_1(t)$	surface conc. of gp41 bound unstably to mAb or Fab at time t (number/cm^2)
$E_T(t)$	surface conc. of gp41 bound stably to mAb or Fab at time t (number/cm^2)
k_{+e}	forward rate const. for Fab binding from solution to a MPER ($M^{-1}s^{-1}$)
k_{-e}	reverse rate const. for Fab dissociating from an MPER (s^{-1})
k_{+1}	forward rate const. for lipid bound Fab binding to MPER (cm^2s^{-1})
k_{-1}	reverse rat cont. for Fab surface dissociation from MPER (s^{-1})
κ_{+d}	rate const. for Fab-MPER bound complex to transition to a stable state (s^{-1})
κ_{-d}	rate const. for stably bound Fab-MPER complex to return to unstable state (s^{-1})
δ	effective forward rate constant for the formation of a mAb-MPER long-lived complex ($M^{-1}s^{-1}$)
d_T	rate at which a bound Fab disables a gp41 (s^{-1})
K_2	equil. constant for a mAb with one site bound to bind to the membrane (cm^2)
L	surface conc. of lipid binding sites recognized by the Fab (cm^{-2})
N	initial number of gp41 bridging the virus and target cell
p_{cell}	probability a virus-target complex bridged by N gp41 will be prevented from fusing
γ_i	parameter defined by Eq. (14) that is a measure of the ease of disabling the ith bond
σ	parameter defined by Eq. (17) that is a measure of the strength and number of gp41 attachments

doi:10.1371/journal.pcbi.1003431.t001

time that an Fab is required to remain bound to an epitope to disable it, $1/d_T$.

$$\delta = \frac{3d_T(k_{+e}\kappa_{+d})}{\kappa_{-d}k_{-e} + d_T(k_{-e}+\kappa_{+d})} \tag{8}$$

Note that when $\kappa_{+d}=0$, $\delta=0$, and therefore $p_b=0$. This is because in the model the Fab or mAb can only disable the epitope after it makes a conformational change to a stably bound configuration, and the rate at which this conformational change occurs is κ_{+d}.

The faster the epitope is disabled the higher will be the probability of preventing fusion. From Eq. (8), a sufficient requirement to achieve maximal disabling of the epitope by the antibody is that $d_T(k_{-e}+\kappa_{+d}) \gg \kappa_{-d}k_{-e}$ or equivalently that

$$d_T \gg \frac{\kappa_{-d}}{1+\kappa_{+d}/k_{-e}} \tag{9}$$

For all the mAbs and Fabs in Table 1, $\kappa_{+d}/k_{-e} < 0.3$, so the condition for maximal disabling, Eq. (9), reduces to requiring that $d_T \gg \kappa_{-d}$.

Table 2. Parameters used to calculate p_b.

Ligand	$k_{+e}(M^{-1}s^{-1})$	$k_{-e}=\bar{k}_{-1}(s^{-1})$	$\kappa_{+d}(s^{-1})$	$\kappa_{-d}(s^{-1})$	$\delta^{max}(M^{-1}s^{-1})$
4E10 Fab	1.0×10^5	0.06	0.012	1.32×10^{-3}	5.0×10^4
4E10 IgG	1.9×10^5	0.15	0.02	1.5×10^{-3}	6.7×10^4
2F5 Fab	1.1×10^5	0.16	0.01	1.81×10^{-3}	1.9×10^4
2F5 IgG	5.1×10^5	0.15	0.05	3.3×10^{-3}	3.8×10^5

The rate constants are from the SPR experiments in Figure 3 of Alam et al. [4]. In these experiments Fab or mAb binds from solution to peptide-liposome conjugates. The best fit is obtained with a two-step conformational change model. The forward and reverse rate constants k_{+e} and k_{-e} characterize the encounter complex step. The forward and reverse rate constants κ_{+d} and κ_{-d} characterize the docking step. When d_T, the rate at which triplets of gp41 are rendered nonfunctional, is much faster than κ_{-d}, d_T no longer enters the calculation. The parameter δ^{max} is calculated from Eq. (10).

doi:10.1371/journal.pcbi.1003431.t002

For a Fab to be effective in neutralizing, as Fabs of 4E10 and 2F5 are [8,9], the model requires that $d_T \gg \kappa_{-d}$, i.e., the time it takes to disable an epitope must be much shorter than the time a Fab remains bound to the epitope. From Table 2 we see this requires that $d_T \gg 0.001\ \mathrm{s}^{-1}$, i.e., disabling must occur in five minutes or less. In Figure 2 we plot p_b as a function of λ, for two different Fab concentrations and a series of different values of d_T. Figure 2 demonstrates that when $d_T \gg 0.001\ \mathrm{s}^{-1}$, p_b becomes independent of d_T. When $d_T \gg \kappa_{-d}$, Eq. (8) becomes

$$\delta^{\max} = \frac{3k_{+e}\kappa_{+d}}{k_{-e}+\kappa_{+d}} \tag{10}$$

Eq. (10) is the limit of Eq. (8) as $d_T \to \infty$, i.e., the instant disabling limit, and therefore, as long as $d_T \gg \kappa_{-d}$, there is no gain achieved in the Fab's ability to disable an epitope by decreasing the time required to disrupt fusion $(1/d_T)$ or by increasing the time the Fab remains bound to the MPER in the stable state $(1/\kappa_{-d})$. In this limit, the rate-limiting step in the disabling of an epitope is the formation of the stably bound antibody-epitope complex, i.e., the bound complex after the epitope has undergone a conformational change.

Eq. (10) shows that $\delta^{\max}$ equals the product of the rate of binding to the epitope, $3k_{+e}$, and the probability that the bound complex will undergo a conformational change rather than breakup, $\kappa_{+d}/(\kappa_{+d}+k_{-e})$. As can be seen from Eq. (7), p_b is determined by the competition between the rate of formation of the stably bound complex, $\delta^{\max}A$, and the rate of fusion, λ. Increasing the affinity of the Fab for the MPER will increase $\delta^{\max}$. Lowering k_{-e} will slow the rate of breakup of the stably bound complex, while increasing k_{+e} will enhance its formation.

In **SI3** of Text S1 we write down and solve the equations for the model when we allow up to three Fab to bind to a single epitope. We show that the results for p_b in the low concentration limit, Eqs. (7) and (10), hold when the Fab concentration satisfies the inequality:

$$A \ll \frac{(\kappa_{+d}+k_{-e})^2}{2k_{-e}k_{+e}} \tag{11}$$

For the rate constants in Table 2 we have that this inequality holds when $A \ll 4.3\times10^{-7}$ M for 4E10 Fab and 8.2×10^{-7} M for 2F5 Fab. Since 50% neutralization (IC_{50}) is typically in the range of 1–50 nM [8–10], we expect the simple expression we previously derived for p_b, Eqs. (7) and (10), to give an excellent description up to these concentrations. Figure 3, for 4E10 Fab, shows a comparison between the predictions for the low concentration limit and the full model. Agreement is excellent for Fab concentrations less than 5×10^{-7} M.

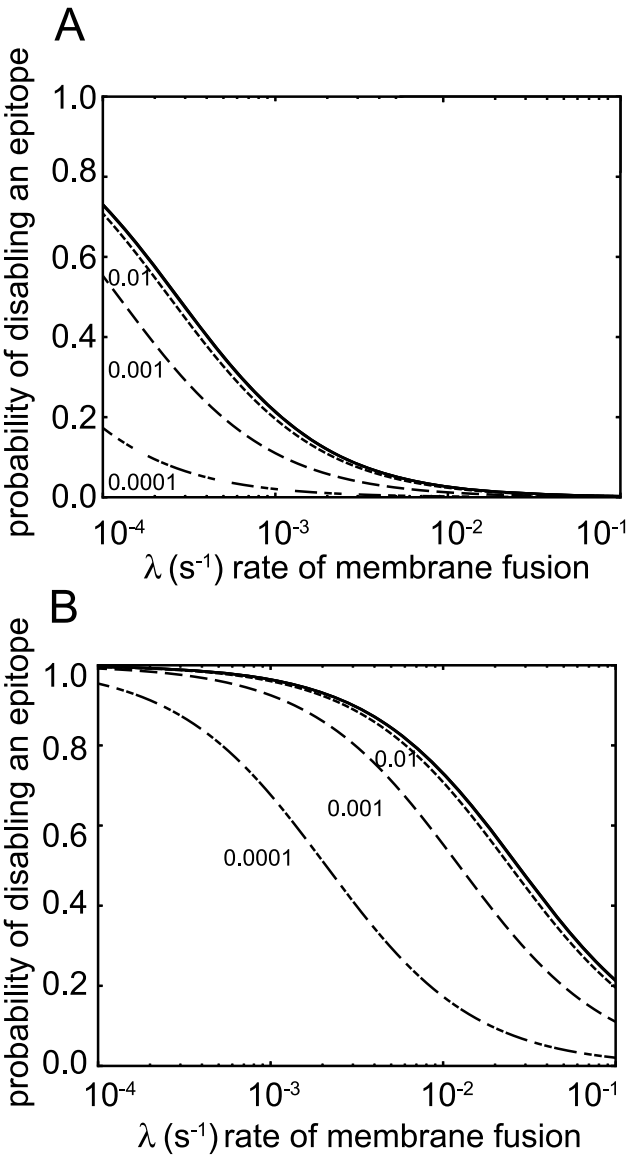

Figure 2. The probability of disabling an epitope, p_b, versus the rate at which membrane fusion occurs, λ, for different values of the disabling rate, d_T. The probability was calculated from Eqs. (7) and (8) for two different 4E10 Fab concentrations, 5×10^{-9} M in A and 5×10^{-7} M in B, using the parameter values given in Table 2. The values of d_T in s^{-1} used to generate the various curves are given in the figures. The curves for $d_T \geq 0.1\ \mathrm{s}^{-1}$ are indistinguishable. The top curves (solid black) in A and B each correspond to three curves generated for $d_T = 0.1\ \mathrm{s}^{-1}$, $1.0\ \mathrm{s}^{-1}$ and $\infty\ \mathrm{s}^{-1}$.
doi:10.1371/journal.pcbi.1003431.g002

Inhibition by polyreactive IgG

In the model we assume that at most one IgG can bind an epitope even though it is composed of three gp41 molecules [28]. In addition, we assume that an IgG can't cross-link two different epitopes. On average the distance between epitopes on HIV-1 is too far for an antibody to span [30]. It has been argued that this allows HIV-1 to evade the effects of antibody avidity and prevent antibodies from forming long-lived attachments by cross-linking different epitopes on the viral surface [31]. However, recent studies show that Env spikes are clustered on mature HIV-1 particles [33]. In the contact region between simian immunodeficiency virus (SIV) and a CD4+ T cell in the prefusion stage, about seven Env spikes are clustered in the contact region with a center to center distance between 140–170 Å [34]. This was closer than the average spacing of Env spikes in unbound SIV ($\sim$200 Å) and comparable to the span between two Fab sites on an IgG (110−150 Å [35,36]).

The binding reactions that the IgG can undergo in the model, and the rate constants that determine the kinetics of the model, are shown in Figure 4. In Figure 4A the IgG cannot bind membrane alone. In Figure 4B the IgG first binds to a lipid site in the membrane with equilibrium constant K_L and then, through a surface reaction, binds to the MPER. The IgG can have only one

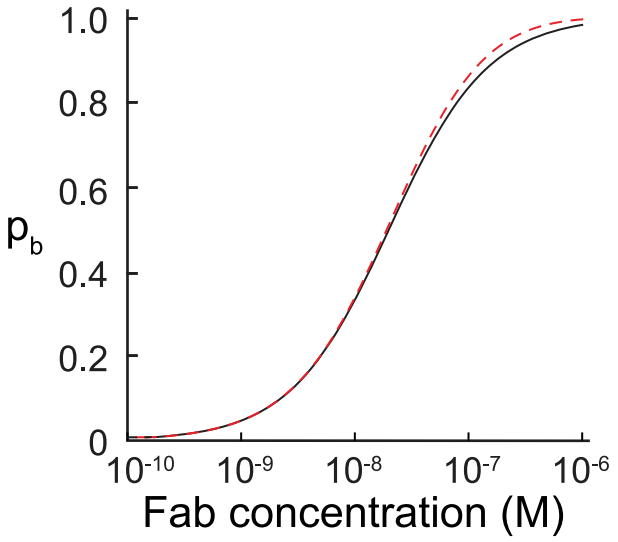

Figure 3. Comparison of the predictions for p_b of the model in the low concentration limit that allows only one Fab to bind per spike (red dashed curve) with the model that allows up to three Fab to bind per spike (solid black curve). The parameters are from Table 1 for 4E10 Fab with $\lambda = 0.001\ s^{-1}$.
doi:10.1371/journal.pcbi.1003431.g003

of its Fab bound to lipid or it can attach to lipid with both its Fab binding sites (A_2 in Figure 4B). It forms the second bound site with an equilibrium cross-linking constant K_2. In addition, if it is bound to the MPER with one site free, that site can also bind to the lipid with equilibrium cross-linking constant K_2 (E_1^* and E_T^* in Figure 4B).

The equations that describe the model in Figure 4B are given in **SI4** of Text S1. There we show that these equations can be reduced to the same set of equations that describe the model for Fab, Eqs. (7) and (10), with the one change, that for IgG the forward rate for binding

$$k_{+e}^{\mathrm{IgG}} = 2k_{+e}^{\mathrm{Fab}}(1 + K_2 L) \tag{12}$$

where k_{+e}^{Fab} is the forward rate constant for an Fab to bind to an MPER and L is the concentration of lipid sites in the membrane. For models where the Fab cannot bind to lipid in the absence of the MPER, $K_2 = 0$, and therefore $k_{+e}^{\mathrm{IgG}} = 2k_{+e}^{\mathrm{Fab}}$. The factor of two arises because for the same molar concentration an IgG has twice as many binding sites as a Fab. In the model, because cross-linking between epitopes is prohibited, the only avidity effects come from the formation of doubly bound antibodies with either both sites bound to lipid or one site bound to a MPER and one to lipid.

2F5 and 4E10 differ in their ability to form bivalent attachments

The avidity effect is characterized by the term K_2L. For the values in Table 1, $K_2L \approx 0$ for 4E10, indicating that there are essentially no 4E10 IgG that have both sites bound to lipid on the liposome-peptide conjugates used in the experiments of Table 2 [4], nor are there any IgG with one site bound to a MPER and the other to lipid. For 2F5 $K_2L \approx 1.3$, or about 40% of the 2F5 IgG that are bound to lipid and not MPER peptide are doubly bound. (This follows because $A_2 = (K_2L/2)A_1$ in Figure 4.) In addition we would expect in the absence of fusion that there would be 1.3 times more 2F5 IgG bridging an MPER and a lipid site than bound to

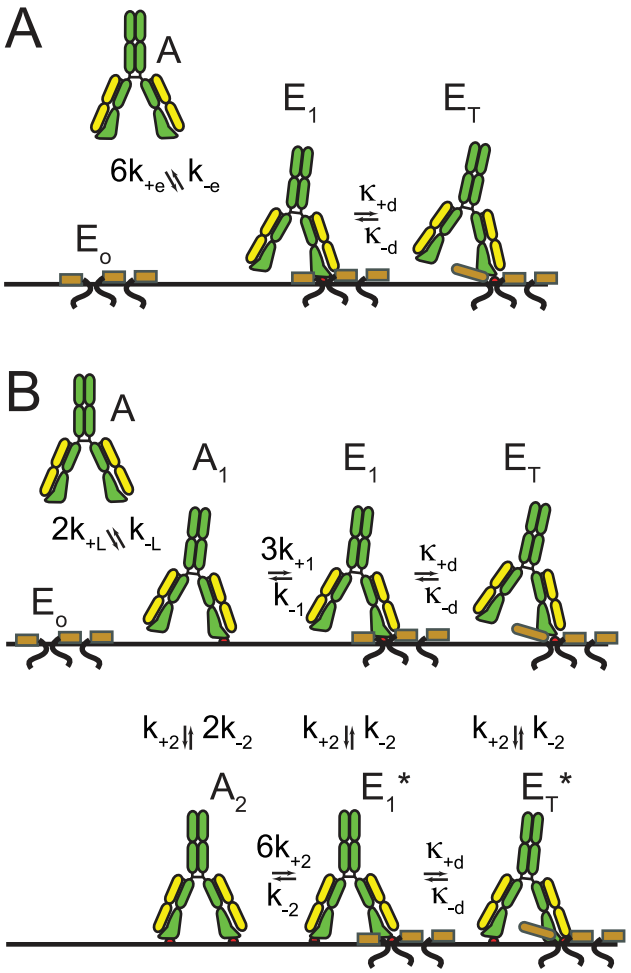

Figure 4. Binding scheme for a polyreactive antibody. A. The binding reactions when the antibody binding sites cannot bind directly to lipids in the membrane. B. The binding reactions when the antibody first binds to lipid in the membrane and then interacts with the MPER. $K_2 = k_{+2}/k_{-2}$ is the surface equilibrium cross-linking constant for an antibody with one site free and one site bound to the membrane or the MPER binding to the membrane to form a bivalent attachment.
doi:10.1371/journal.pcbi.1003431.g004

MPER alone. We note that the value of K_2L may be an over estimate since these experiments were done on peptide-liposome conjugates and some cross-linking of the MPER peptides may have occurred.

The picture that 2F5 interacts more stably than 4E10 with membrane lipid is in agreement with previous experiments. SPR studies of 4E10 and 2F5 binding to liposomes without peptide (Figure 3A and 3B in [4]) indicate that bound 2F5 dissociates more slowly from the liposomes than bound 4E10. Also 2F5 was found to bind to virus-like particles bearing no envelop glycoprotein while such binding could not be detected with 4E10 [6]. This is consistent with 4E10 being described by the wedging model and 2F5 by the encounter model [13].

From the values we obtained for K_2L, we predict that in a neutralization experiment 4E10 IgG and Fab should be similarly effective when the concentration per mole of Fab sites is the same, while we predict the opposite for 2F5. Shown in Figure 5 are neutralization experiments for 4E10 and 2F5 Fab and IgG, plotted as a function of the molar concentration per Fab site. Figure 5A and 5B show that unlike 2F5, 4E10 IgG is only marginally more

effective than its Fab fragment. The inserts in A and B of Figure 5 are the predicted values of p_b for the parameters given in Table 1. These parameters were determined from SPR binding studies to peptide-liposome conjugates, while the neutralization studies used pseudotyped virus, and therefore neither the membrane composition nor the manner in which the epitope was displayed on the membrane was the same. None-the-less, the qualitative prediction is born out. For the same concentration of Fab sites, in a neutralizing experiment 2F5 IgG is much more effective than its Fab compared with 4E10 IgG and its Fab as has previously been observed [36]. From Table 1 we see the value of δ for 2F5 is greater than for 4E10. Therefore, the model predicts that 2F5 will be more effective at neutralization than 4E10. Neutralization experiments that use either 2F5 or 4E10 mAb, shown in Figure 5C, agree with this prediction.

Modeling neutralization

For mAbs and Fab that bind epitopes within the MPER we have derived an expression for the probability, p_b, of disabling an epitope on a virion that is bound to a target cell, Eqs (7) and (10), as a function of the Fab or IgG concentration. In deriving p_b we assumed that there was a uniform distribution of N gp41 trimers bridging the virus and target cell and that N was sufficiently large that p_b was independent of N. An obvious question is, how is this probability related to the fraction of target cells prevented from being infected in a neutralization assay? For a virion that initially has N epitopes bound to a target cell, and to prevent fusion all N must be disabled, we propose that the probability of preventing fusion is

$$p_{\text{cell}} = p_N p_{N-1} \cdots p_i \cdots p_2 p_1 \tag{13}$$

where p_i is the probability a bond in the presence of $i-1$ other bonds is disabled before it fuses. Writing p_{cell} as a product of N different probabilities assumes that the individual probabilities are independent, i.e., each individual probability depends only on the number of bonds present that bridge the virus and target cell and not on what has happened previously. Writing p_{cell} in this way also recognizes the possibility that the number of gp41 trimers bridging the region between virion and target cell influences the probability of a bond rupturing before fusion. In general cellular membranes repel each other as a result of nonspecific forces that fall off with the distance between the membranes [37]. For the membranes to attach, specific bonding is required to overcome the repulsive forces. The bonds that hold the two membranes together are under stress with the bonds at the edge of the contact region between the two membranes experiencing larger stresses than those in the interior of the contact region [38]. For this reason we expect that when there is one or only a few bonds present there will be increased strain on a bond and as a result it will be more easily disabled by a mAb then when a bond is surrounded by many other bonds as illustrated in Figure 6.

Models have been presented to determine the stoichiometry of entry T, defined as the number of attached gp41 trimers required to infect the target cell [32,39,40]. Although this parameter is not defined in our model, our model encompasses the stoichiometry of entry. For example, if in Eq. (13) we have that $p_1 \approx p_2 \approx 1$ and $p_3 < 1$, then $T = 3$. If the virion and target cell are attached by three trimers, if one of those trimers is disable, the two remaining trimers will spontaneously disable. The stoichiometry of entry has yet to be rigorously determined, but it is most probably greater than one [32].

To analyze neutralization experiments we treat the population of virion-target cell complexes as if they were homogeneous, each held together with the same number of bonds at the start of the experiment. We also assume that each target cell has at most one HIV-1 bound to it. Since p_{cell} is the probability of a target cell not becoming infected when bound to a virion in the presence of an antibody concentration A, it also equals the fraction of target cells in a neutralization assay that are prevented from being infected at antibody concentration A.

To proceed we need to obtain an expression for p_i as function of i and of A. We do this by assuming a form for p_i that has the following limiting behavior: when the number of bonds is large, p_i is independent of i and equal to p_b; When the number of bonds is small, p_i is elevated (more easily disabled) compared to p_b.

$$p_i = p_b^{\gamma_i} = \left(\frac{\delta A}{\lambda + \delta A}\right)^{\gamma_i} \tag{14}$$

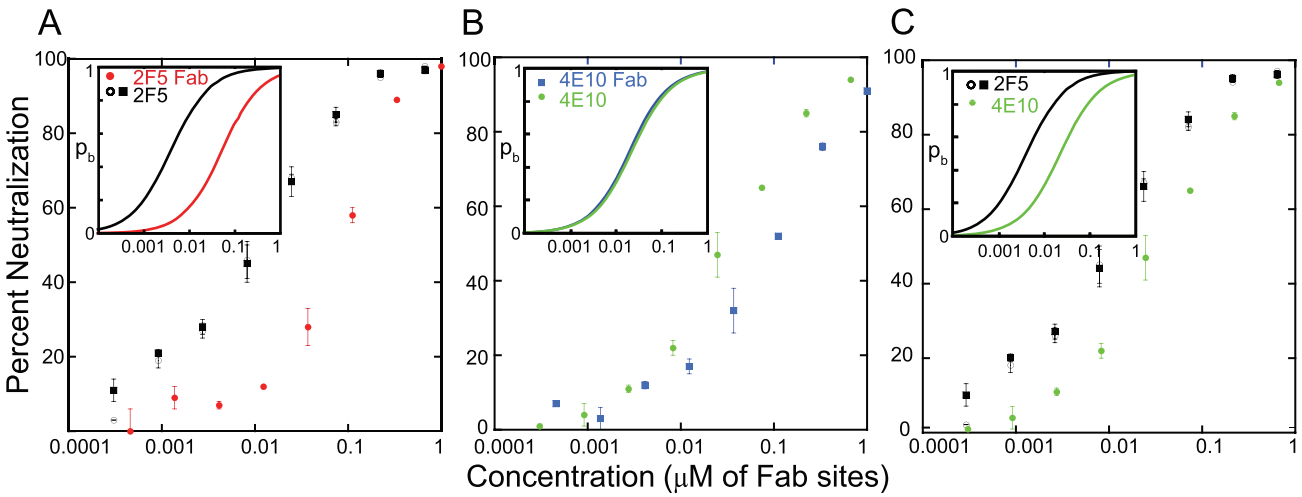

Figure 5. Neutralization of HIV-1 pseudovirus by Fab and IgG 2F5 and 4E10. The fraction neutralized is plotted against the concentration of Fab sites. The inserts in A, B and C are the calculated values of p_b from Eq. (7) and (10) versus the concentration of Fab sites for $\lambda = 0.001\ \text{s}^{-1}$ and the parameters given in Table 2. Neutralization by A. 2F5 Fab (red circles) and two preparations of 2F5 IgG (solid squares and open circles), B. 4E10 Fab (blue squares) and 4E10 IgG (green circles), and C. 2F5 IgG from panel A and 4E10 IgG from panel B.
doi:10.1371/journal.pcbi.1003431.g005

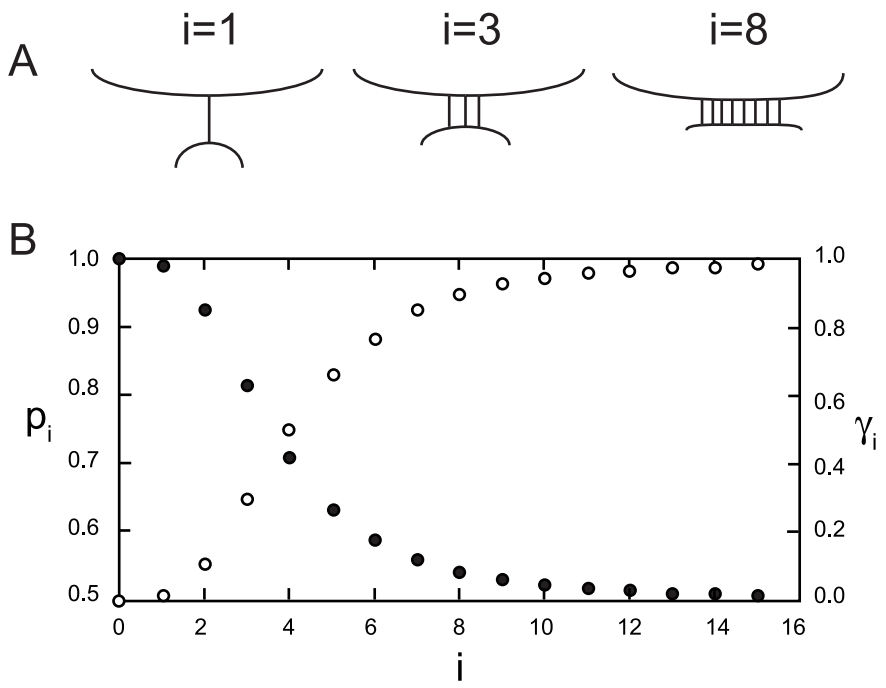

Figure 6. An example of how the probability p_i of disabling a bond when there are i bonds present might depend on i. A. Because of the repulsive forces between membranes, when a single bond bridges two membranes it will be stretched further than a bond that is one of many holding the membranes together. B. In this example the probability of breaking a bond in the presence of a large number of other bonds $p_b = 0.5$, $p_i = p_b^{\gamma_i}$ (closed circles), Eq. (14), and σ_i (open circles) was calculated from Eq. (15) with $\beta = 2$ and $n = 4$. The values obtained for p_i are given in Table 3.
doi:10.1371/journal.pcbi.1003431.g006

where $0 \le \gamma_i \le 1$. When $\gamma_i = 1$, $p_i = p_b$ and p_i is independent of the number of bonds present, while when $\gamma_i = 0$, $p_i = 1$ and the ith bond breaks spontaneously. To help us interpret our results in the next section when we analyze neutralization experiments, it will be useful to have a concrete expression for γ_i. A reasonable choice because of its flexibility, few parameters, and its range between zero and one, is a Hill function which we write as follows:

$$\gamma_i = \frac{(i/n)^\beta}{1+(i/n)^\beta} \tag{15}$$

In Figure 6, γ_i and p_i are plotted for $n = 4$, $\beta = 3$ and $p_b = 0.5$. For any set of parameters, when $i = n$, $\gamma_i = 0.5$ and $p_i = \sqrt{p_b}$. When $i > n$, p_i approaches p_b as i increases. It can be seen from Figure 6 and Table 3 that for these parameters p_1 and p_2 are both greater than 0.9. Therefore, in this example, the last two trimers between virion and target cell have a high probability of spontaneously disabling indicating the stoichiometry of entry $T = 3$.

From Eqs. (13), (14) and (15) we can write p_{cell} in the following form:

$$p_{\text{cell}} = \left(\frac{\delta A}{\lambda + \delta A}\right)^\sigma \tag{16}$$

where

$$\sigma = \sum_{i=1}^{N} \gamma_i \tag{17}$$

and $0 \le \sigma \le N$.

Properties of the IC_{50}

It is useful to rewrite p_{cell} in terms of the IC_{50}, the antibody concentration at which 50% of the virion-target cell complexes do not go on to fuse. In terms of the IC_{50}, Eq. (16) becomes

$$p_{\text{cell}} = \left(\frac{A/IC_{50}}{\alpha + A/IC_{50}}\right)^\sigma \tag{18}$$

where

$$\alpha = e^{\ln 2/\sigma} - 1 \tag{19}$$

and

$$IC_{50} = \frac{\lambda}{\delta\alpha} \tag{20}$$

Table 3. The values of p_i (Eq. (14)), γ_i (Eq.(15)), and σ for the example in Figure 6.

i	p_i	γ_i	N	$\sigma = \sum_{i=1}^{N} \gamma_i$
1	0.9894	0.0154	1	0.0154
2	0.9259	0.1111	2	0.1265
3	0.8141	0.2967	3	0.4232
4	0.7071	0.5000	4	0.9232
5	0.6323	0.6614	5	1.6946

doi:10.1371/journal.pcbi.1003431.t003

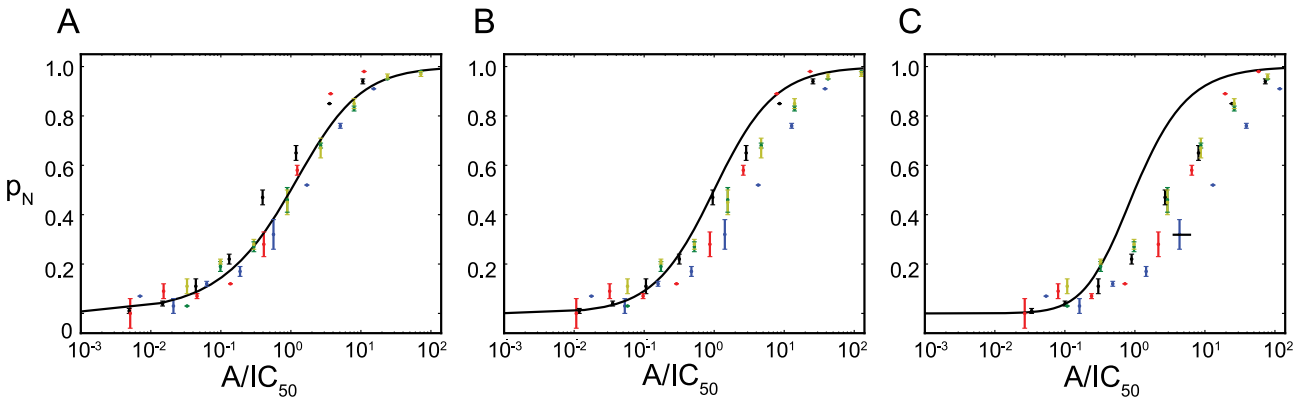

Figure 7. Fit of the model to the four neutralization experiments shown in Figure 5. A. A global nonlinear least squares fit was performed, fitting Eq. (18) to the four experiments with five free parameters, four IC_{50} and σ. The best fit values obtained were: $\sigma = 0.64 \pm 0.11$, and for the IC_{50} values in μg/ml, 4E10 IgG = 4.3 ± 1.6, 4E10 Fab = 3.3 ± 1.0, 2F5 IgG = 0.68 ± 0.18, and 2F5 Fab = 4.5 ± 1.5. The neutralization data is plotted versus A/IC_{50} using the determined IC_{50} values. The solid curve is p_{cell}, given by Eq. (18), with $\sigma = 0.64$ and the best fit values for the four IC_{50}. In B and C, σ was fixed at $\sigma = 1$ and $\sigma = 2$ respectively and only the four IC_{50} values were varied. The neutralization data is plotted versus A/IC_{50} using the determined IC_{50} values for the fixed values of σ.
doi:10.1371/journal.pcbi.1003431.g007

The parameter α was chosen so that $p_{cell} = 1/2$ when $A = IC_{50}$. It is a decreasing function of σ that is equal to one when $\sigma = 1$. Eq. (18) predicts the following dependencies of IC_{50} on the parameters of the model: The faster fusion occurs (larger λ) the higher IC_{50}; the more bonds required to be disabled (larger σ and therefore smaller α) the higher IC_{50}; and the more rapidly the antibody binds to the epitope and induces a stable complex (larger δ) the lower IC_{50}.

Note that the IC_{50} is inversely proportional to δ. Since we have an expression for how δ depends on the binding parameters, Eq. (10), using the values obtained from SPR data (Table 2), we can predict how the IC_{50} will shift as a result of modifying the rate constants. For example, increasing the mAb affinity by decreases k_{-e} by a factor of ten is predicted to lower the IC_{50} for mAbs 4E10 and 2F5 by factors of 4.86 and 3.1 respectively. Since k_{+e} is directly proportional to δ^{max}, increasing the mAb affinity by increasing k_{+e} by a factor of ten is predicted to lower the IC_{50} for both mAbs by a factor of ten.

Analyzing neutralization experiments

Eq. (18) predicts that if a series of neutralizing experiments are performed under the same conditions with different mAbs or Fabs, and the fraction of target cells neutralized is plotted against A/IC_{50}, all the experiments should lie on the same curve. To test this prediction we use the four neutralization experiments shown in Figure 5. We simultaneously fit the four neutralization experiments with five free parameters, four IC_{50} and σ, that we take to be the same in all experiments. As can be seen in Figure 7A, when plotted as a function of A/IC_{50} the four experiments lie on a universal curve. Figure 7A gives a best fit value for $\sigma = 0.64 \pm 0.11$, where the error bounds are the 95% confidence interval obtained from bootstrapping. Using other parameter estimation methods to simultaneously fit the four neutralization experiments, as discussed in **SI5** of Text S1, give similar values for σ. When we fit each experiment separately σ ranged from 0.45 to 1.15 with an average $\sigma = 0.77 \pm 0.15$. Figures 7B ($\sigma = 1$) and 7C ($\sigma = 2$) show that the fits get progressively worse with increasing σ.

To interpret the value of σ that we have obtained, it is instructive to consider the example in Figure 6. As can be seen from Table 3, a $\sigma = 0.64 \pm 0.11$ in this example would mean that initially there were between three ($\sigma = 0.42$) and four ($\sigma = 0.92$) bonds attaching the virus and target cell with the last bond, $i = 1$, breaking spontaneously ($p_1 = 0.99$). Since for our experimental system we don't know the values of n and β, we can't calculate the values of γ_i and determine the σ closest to our best fit value of 0.64. However, we do know that when $i = n$, $\gamma_i = 0.5$ so for our σ value, the γ_i values for $i < n$ must be small. This suggests that as in our example, $\sigma = 0.64 \pm 0.11$ corresponds to the total number of gp41 attachments at the start of the experiment $N \leq n$. The bond n marks a transition. For $i < n$ the bonds are highly strained and as a result more easily disabled than when $i > n$.

Discussion

The probability of disabling a trivalent gp41 in the pre-hairpin intermediate depends on a number of factors including the concentration of mAb available to bind to gp41 and the number of gp41 bridging the virus and target cell. We expect that for a fixed antibody concentration, as the number of gp41 attachments increases, the probability decreases (it becomes harder to disable a bond) reaching a plateau where the probability (p_b in our model) is independent of the number of bonds present. In this limit, increasing the number of bonds increases the contact area between virus and target cell while the bond density remains uniform [37]. For this limit we presented a kinetic model and used it to calculate, for a given concentration A of polyreactive mAbs or Fabs, the probability that during the pre-hairpin intermediate, a trivalent gp41 will be rendered incapable of completing the fusion process when a single Fab or mAb binds to one of the three exposed MPERs. The model predicted that for the antibody to be effective in neutralizing HIV-1, the time it takes to disable an epitope must be shorter than the time the epitope remains in the long-lived conformation induced by antibody binding. For 4E10 and 2F5, whose dissociation rate constants for the breakup of the long-lived complex $\kappa_{-d} \approx 10^{-3}$ s^{-1} (Table 1 and [4,17]), the time to disable an epitope must be about five minutes or less. Increasing the time the antibodies remain bound in the long-lived conformation (lowering κ_{-d}) would not improve their neutralization capabilities. Rather, it is the rate of formation of the long-lived conformation that is the limiting step in determining the ability of these antibodies to disable epitopes. The effective forward rate constant for this step, the parameter δ^{max} in the model, given by Eq. (10),

equals the product of the forward rate constant for binding of the antibody in solution to the epitope, k_{+e}, and the probability that the bound complex undergoes a conformational change rather than dissociating, $\kappa_{+d}/(k_{-e}+\kappa_{+d})$. In the encounter model, which we believe well characterizes the kinetics of binding of 2F5, k_{+e} is the overall rate constant for the binding of the antibody from solution to the membrane, diffusion of the membrane bound antibody to the epitope, and binding of the antibody to the epitope through a surface reaction. Increasing the antibody's affinity for the membrane or its affinity for the MPER is predicted to result in higher values of δ^{max}, higher values for the probability of disabling an epitope and lower values for the IC_{50}. Increasing the affinity of the antibody by lowering its dissociation rate constant for the MPER, k_{-e}, will increase the probability of forming a long-lived complex, while increasing the affinity by increasing the forward rate constants will increase the rate of formation of the initial antibody-MPER complex.

From previous SPR studies of 2F5 and 4E10 Fab and IgG binding to peptide-lipisome conjugates [4] we determined the values of $\delta^{\max}$ for these four ligands. These values led us to predict that 2F5 IgG would exhibit a much stronger avidity effect than 4E10 IgG. The prediction was tested by comparing neutralization experiments using Fab and IgG and plotting the ligand concentration in Fab sites per mole. If there were no avidity effect, such a plot should yield two identical curves. In the plots in Figure 5A and 5B the prediction was born out. The mAb 2F5 was much more effective than its Fab, while the mAb 4E10 was only marginally better than its Fab. In the model the strong avidity of 2F5 IgG arises as result of its being able to form cross-links between the MPER and the viral membrane. This result is consistent with experiments showing that 2F5 interacts more stably with the viral membrane than does 4E10 [6]. We cannot rule out that an additional contribution to the avidity comes from the mAb cross-linking different MPERs on the same virion, something not in the model. Indeed, in light of recent studies showing that Env spikes are clustered on mature HIV-1 [33], and because 2F5 and 4E10 interact with gp41 after it has attached to the target cell membrane and clustered in the contact region between the two membranes, it is to be expected that some cross-linking of MPERs occurs. Still, 4E10 shows little improvement over its Fab in neutralization, indicating that for 4E10 there is little or no cross-linking of MPERs. In contrast, 2F5 shows a high avidity, but what contribution, if any, comes from 2F5 cross-linking two MPERs rather than MPER and viral membrane, is unknown.

Although, the model we presented to calculate p_b delineated the roles of the rate constants in determining the ability of 2F5 and 4E10 to disable an epitope, it couldn't be directly applied to analyze neutralization experiments. To do this we considered an HIV and target cell bridged by N gp41 at the start of a neutaliation experiment and asked the question, what is the probability of sequentially disabling all N gp41s before one of them fused? To answer this question required a model that quantified the influence of the number of bridging bonds on bond breakage. We proposed an expression for p_i, the probability of disabling a bond when i bonds are present, given by Eq. (14). The expression was chosen so that it had the correct limiting behavior, that when i was large p_i was independent of i and when i was small the probability of disabling increased as the bonds came under additional strain. Using this expression for p_i we were able to obtain an expression for the probability of disabling all N bonds before fusion occurred, Eq. (18).

One prediction of the model, Eq. (20) is how the IC_{50} depends on the model parameters. For a mean time of fusion of 10–30 min ($\lambda = 0.0006-0.0017\ \mathrm{s}^{-1}$) [20–22], $\delta^{\max} = 6.7\times10^4\ \mathrm{M}^{-1}\mathrm{s}^{-1}$, the value for 4E10 in Table 2, and $\alpha = 1.95$, $IC_{50} = 4.8-13.4$ nM. For $\delta^{\max} = 3.8\times10^5\ \mathrm{M}^{-1}\mathrm{s}^{-1}$, the value for 2F5 from Table 1, $IC_{50} = 0.8-2.3$ nM. These predicted values, obtained for values of $\delta^{\max}$ from SPR experiments with peptide-vesicle conjugates, are consistent with the IC_{50} values determined from neutralization experiments [8–11,13,24,28,36,41] and lend some support to the model.

The model also predicted that for a series of neutralization experiments with different mAbs and Fabs, a plot of the fraction of virus neutralized in each experiment versus A/IC_{50}, should lie on a single curve. After we fit Eq. (18) to four experiments that used 2F5 and 4E10 mAb and Fab, and replotted the data as a function of A/IC_{50}, the data did lie on a universal curve (Figure 7A). From the analysis of these data we could not determine the number of gp41 bridging the virus and target cell at the start of the experiment, but the analysis indicated that these bonds are few in number and under considerably more strain then if there were a large number of attachments in the contact region.

There are relatively few Env spikes on HIV-1. The average number has been reported to be between seven and 14 spikes per HIV-1 [30,33,42,43]. Zhu et al. found 14 ± 7 spikes per HIV-1 with a range of four to 35 [30]. Using electron tomography about five to seven spikes have been observed in the contact region between virion and CD+ T cell in the prefusion stage [34]. This was the case when the virion was either SIV or HIV. However, it is not known how many gp41 membrane spanning trimers are established after the loss of gp120 and the entrance into the pre-hairpin intermediate. Attempts have been made to determine the stoichiometry of HIV entry, but as yet reliable estimates of the minimum number of attachments required for fusion to occur have not been established [32,39,40,44]. It therefore remains to be seen whether this picture, where just a few weak attachments are mediating fusion and neutralization can be achieved by disabling these, is a reasonable description of what is occurring in the neutralization experiments we have analyzed.

Materials and Methods

Neutralization assay

Neutralization was determined by monitoring reductions in luciferase reporter-gene expression after a single round of infection by pseudotyped HIV-1 virus in TZM/bl cells, as described previously [45] The Tzm/bl cell neutralization assay was done using 2F5 and 4E10 mAbs and their Fab fragments. Antibodies were preincubated with the pseudovirus for 1 h using a dose titration starting at $50\ \mu\mathrm{g/ml}$ and a series (seven) of 3-fold dilutions.

Parameter estimation

Best fit values for the parameters where obtained using the Common Los Alamos Software Library fitting routine DNLSI which is based on a finite difference Levenberg-Marquardt algorithm for solving nonlinear least-squares problems. Estimates of the 95% confidence intervals were obtained by using the bootstrap method described by Efron and Tibshirani [46]. For each estimate 500 simulations were performed. Increasing the number of simulations caused no significant change in the error estimate. The program that runs under Linux and Mac OS, and is called FUI, can be downloaded from Professor Rob J. de Boer's website, http://www-binf.bio.uu.nl/rdb/software.html. Additional methods, discussed in **SI5** of Text S1, were used to check the parameter estimations.

Supporting Information

Text S1 Supplementary Information in which is presented equations and calculations omitted from the manuscript as well as an expanded discussion of the fitting methods that were used. (PDF)

Author Contributions

Conceived and designed the experiments: SMA HXL. Performed the experiments: SMA HXL. Analyzed the data: BH BG. Contributed reagents/materials/analysis tools: BH HXL SMA BG. Wrote the paper: BG BH. Developed and analyzed the mathematical model: BH BG.

References

1. Verkoczy L, Kelso G, Moody MA, Haynes BF (2011) Role of immune mechanisms in induction of HIV-1 broadly neutralizing antibodies. Curr Opin Immunol 23: 383–390.
2. Frey G, Chen J, Rits-Volloch S, Freeman M, Zolla-Pazner S, et al. (2008) Distinct conformational states of HIV-1 gp41 are recognized by neutralizing and non-neutralizing antibodies. Nat Struct Mol Biol 17: 1486–1492.
3. Zhu Z, Qin HR, Chen W, Zhao Q, Shen X, et al. (2011) Cross-reactive HIV1-neutralizing human monoclonal antibodies identified from a patient with 2F5-like antibodies. J Virol 85: 11401–11408.
4. Alam SM, McAdams M, Boren D, Rak M, Scearce RM, et al. (2007) The role of antibody polyspeci-ficity and lipid reactivity in binding of broadly neutralizing anti-HIV-1 envelope human monolonal antibodies 2F5 and 4E10 to glycoprotein 41 membrane proximal envelope epitopes. J Immunol 22: 4424–4435.
5. Rathinakumar R, Dutta M, Zhu P, Johnson WE, Roux KH (2011) Binding of anti-membraneproximal gp41 monoclonal antibodies CD4-liganded and -unliganded human immuneodeficiency virus type 1 and simian immunodeficiency virus virions. J Virol 86: 1820–1831.
6. Tong T, Crooks ET, Osawa K, Binley JM (2012) HIV-1 virus-like particles bearing pure Env trimers expose neutralizing epitopes but occlude nonneutralizing epitopes. J Virol 86: 3574–3587.
7. Cardoso RMF, Zwick MB, Stanfield RL, Kunert R, Binley JM, et al. (2005) Broadly neutralizing anti-HIV antibody 4E10 recognizes a helical conformation of a highly conserved fusion-associated motif in gp41. Immunity 78: 163–173.
8. Ofek G, Tang M, Sambor A, Katinger H, Mascola JR, et al. (2004) Structure and mechanistic analysis of the anti-human immunodeficiency virus type 1 antibody 2F5 in complex with its gp41 epitope. J Virol 271: 10724–10737.
9. Zwick MB, Wang M, Poignard P, Stiegler G, Katinger H, et al. (2001) Neutralization synergy of human immunodeficiency virus type 1 primary isolates by cocktails of broadly neutralizing antibodies. J Virol 75: 12198–12208.
10. Alam S, Morelli M, Dennison SM, Liao HX, Zhang R, et al. (2009) Role of HIV membrane in neutralization by two broadly neutralizing antibodies. Proc Natl Acad, Sci USA 106: 20234–20239.
11. Ofek G, McKee K, Yang Y, Yang ZY, Skinner J, et al. (2010) Relationship between antibody 2F5 neutralization of HIV-1 and hydrophobicity of its heavy chain third complementarity-determining region. J Virol 84: 2955–2962.
12. Julien JP, Harte N, Maeso R, Taneva SG, Cunningham A, et al. (2010) Ablation of the complementarity-determining region H3 apex of the anti-HIV-1 broadly neutralizing antibody 2F5 abrogates neutralization capacity without affecting core epitope binding. J Virol 84: 4136–4147.
13. Xu H, Song L, Kim M, Holmes MA, Kraft Z, et al. (2010) Interactions between lipids and human anti-HIV antibody 4E10 can be reduced without ablating neutralization activity. J Virol 84: 1076–1088.
14. Yang G, Holl TM, Liu Y, Li Y, Lu X, et al. (2013) Identification of autoantigens recognized by the 2F5 and 4E10 broadly neutralizing HIV-1 antibodies. J Exp Med 210: 241–256.
15. Sun ZYJ, Oh KJ, Kim M, Yu J, Brusic V, et al. (2008) HIV-1 broadly neutralizing antibody extracts its epitope from a kinked gp41 ectodomain region on the viral membrane. Immunity 28: 52–63.
16. Song L, Sun ZYJ, Coleman KE, Zwick MB, Gach JS, et al. (2009) Broadly neutralizing anti-HIV-1 antibodies disrupt a hinge-related function of gp41 at the membrane interface. Proc Natl Acad Sci USA 106: 9057–9062.
17. Dennison SM, Stewart SM, Stempel KC, Liao HX, Haynes BF, et al. (2009) Stable docking of neutralizing human immundeficiency virus type 1 gp41 membrane-proximal external region monoclonal antibodies 2F5 and 4E10 is dependent on the membrane immersion depth of their epitope regions. J Virol 83: 10211–10223.
18. Kim M, Sun ZYJ, Rand KD, Shi X, Song L, et al. (2011) Antibody mechanics on a membrane-bound HIV segment essential for gp41-targeted viral neutralization. Nat Struct Mol Biol 18: 1235–1243.
19. Chan DCD, Kim PSP (1998) HIV entry and its inhibition. Cell 93: 681–684.
20. Muñoz Barroso I, Durell S, Sakaguchi K, Appella E, Blumenthal R (1998) Dilation of the human immunodeficiency virus-1 envelope glycoprotein funsion pore revealed by inhibitory action of a synthetic peptide from gp41. J Cell Biol 140: 315–323.
21. Dimitrov AS, Jacobs A, Finnegan CM, Stiegler G, Katinger H, et al. (2007) Exposure of the membrane-proximal external region of HIV-1 gp41 in the course of HIV-1 envelope glycoproteinmediated fusion. Biochemistry 46: 1398–1401.
22. Haim H, Steiner I, Panet A (2007) Time frames for neutralization during the human immunodeficiency virus type 1 entry phase, as monitored in synchronously infected cell cultures. J Virol 81: 3525–3534.
23. Miyauchi K, Kozlov MM, Melikyan GB (2009) Early steps of HIV-1 fusion define the sensitivity to inhibitory peptides that block 6-helix bundle formation. Plos Pathog 5: e1000585.
24. Chakrabarti BK, Walker LM, Guenaga JF, Poignard P, Burton DR, et al. (2011) Direct antibody access to the HIV-1 membrane-proximal external region positively correlates with neutralization sensitivity. J Virol 85: 8217–8226.
25. Shen X, Dennison SM, Liu P, Gao F, Jaeger F, et al. (2010) Prolonged exposure of the HIV-1 gp41 membrane proximal region with L669S substitution. Proc Natl Acad Sci USA 107: 5972–5977.
26. Steger HK, Root MJ (2006) Kinetic dependence to HIV-1 entry inhibition. J Biol Chem 281: 25813–25821.
27. Ruprecht CR, Krarup A, Reynell L, Mann AM, Brandenberg OF, et al. (2011) MPER-specific antibodies induce gp120 shedding and irreversible neutralize HIV-1. J Exp Med 208: 439–454.
28. Crooks ET, Jiang P, Franti M, S W, Zwick MB, et al. (2008) Relationship of HIV-1 and SIV envelope glycoprotein trimer occupation and neutralization. Virology 377: 364–378.
29. Kim M, Chen B, Hussey RE, Chishti Y, Montefiori D, et al. (2001) The stoichiometry of trimeric SIV glycoprotein interaction with CD4 differs from that of anti-envelope antibody Fab fragments. J Biol Chem 276: 42667–42676.
30. Zhu P, Liu J, Chertova E, Bess J, Lifson J, et al. (2006) Distribution and three-dimensional structure of AIDS virus envelope spikes. Nat Cell Biol 441: 847–852.
31. Klein JS, Bjorkman PJ (2010) Few and far between: how HIV may be evading antibody avidity. Plos Pathog 6: e1000908.
32. Magnus C, Rusert P, Bohoeffer S, Trkola A, Regoes RR (2009) Estimating the stoichiometry of human immunodeficiency virus entry. J Virol 83: 1523–1531.
33. Chojnacki J, Staudt T, Glas B, Bingen P, Engelhardt J, et al. (2011) Maturation-dependent HIV-1 surface protein redistribution revealed by fluorescence nanoscopy. J Virol 338: 1820–1831.
34. Sougrat R, Bartesaghi A, Lifson JD, Bennett AE, Bess JW, et al. (2007) Electron tomography of the contact between T cells and SIV/HIV: Implications for viral entry. Plos Pathog 3: 524–528.
35. Sosnick TR, Novotay BJ, Seeger PA, Trewhella J (1992) Distances between the antigen-binding sites of three murine antibody subclasses measured using neutron and X-ray scattering. Biochemistry 31: 1779–1786.
36. Klein JS, Gnanapragasam PNP, Galimidi RP, Foglesong CP, West JAP, et al. (2009) Examination of the contributions of size and avidity to the neutralization mechanisms of the anti-HIV antibodies B12 and 4E10. Proc Natl Acad Sci USA 106: 7385–7390.
37. Bell GI, Dembo M, Bongrand P (1984) Cell adhesion: Competition between nonspecific repulsion and specific bonding. Biophys J 45: 1051–1064.
38. Dembo M, Torney DC, Saxman K, Hammer D (1988) The reaction-limited kinetics of membraneto- surface adhesion and detachment. Proc Royal Soc Lond B 234: 55–83.
39. Magnus C, Regoes RR (2010) Estimating the stoichiometry of HIV neutralization. PLoS Comp Biol 6: e1000713.
40. Magnus C, Regoes RR (2012) Analysis of the subunit stoichiometries in viral entry. PLoS ONE 7: e33441.
41. Zwick MB, Komori H, Stanfield RL, Church S, Wang M, et al. (2004) The long third complementarity-determining region of the heavy chain is important in the activity of the broadly neutralizing anti-human immunodeficiency virus type 1 antibody 2F5. J Virol 78: 3155–3161.
42. Chertova E, Bess Jr JW, Crise BJ, Sowder II RC, Schaden TM, et al. (2002) Envelope glycoprotein incorporation, not shedding of surface envelope glycoprotein (gp120/SU), is the primary determinant of SU content of purified human immunodeficiency virus type 1 and simian immunodeficiency virus. J Viro 76: 5315–5325.
43. Zhu P, Liu J, Bess J, Chertova E, Lifson J, et al. (2003) Electron tomography analysis of envelope glycoprotein trimers on HIV and simian immunodeficiency virus virions. Proc Natl Acad Sci USA 100: 15812–15817.
44. Klasse PJ (2012) The molecular biology of HIV entry. Cell Microbiol 14: 1183–1192.
45. Liao HK, Sutherland LL, Xia SM, Brock ME, Scearce RM, et al. (2006) A group M consensus envelope glycoprotein induces antibodies that neutralize subsets of subtype B and C HIV-1 primary viruses. Virology 353: 268–282.
46. Efron B, Tibshirani R (2006) Bootstrap methods for stander errors, confidence intervals, and other measures of statistical accuracy. Stat Sci 1: 54–75.